

# Direct correlation between the near-proton-emission threshold resonance in $^{11}\text{B}$ and the branching ratio of beta-delayed proton emission from $^{11}\text{Be}$

Nguyen Le Anh\*

*Department of Physics, Ho Chi Minh City University of Education,  
280 An Duong Vuong, District 5, Ho Chi Minh City, Vietnam*

Bui Minh Loc†

*San Diego State University, 5500 Campanile Drive, San Diego, CA 92182*

(Dated: November 19, 2024)

**Background:** Beta-delayed proton emission from neutron halo nuclei  $^{11}\text{Be}$  represents a rare decay process. The existence of the narrow resonance near the proton-emission threshold in  $^{11}\text{B}$  explains its unexpectedly high probability. However, the accurate value of the branching ratio remains challenging to determine.

**Purpose:** We aim to provide a microscopic potential model to determine the branching ratio for beta-delayed proton emission from  $^{11}\text{Be}$ . We focus on quantifying the influence of the narrow resonance near the proton emission threshold on the result of the branching ratio.

**Method:** We employ the Skyrme Hartree-Fock calculation within the potential model to obtain the branching ratio. We derive the single-particle potentials for the halo neutron and the emitting proton from the Skyrme Hartree-Fock calculation with minimal adjustment. As the resonance position is tightly linked to the potential depth, we can demonstrate quantitatively how variations in its location impact the outcome.

**Result:** Slight variations in the resonance position significantly impact the branching ratio, with the upper limit reaching the order of  $10^{-5}$ .

**Conclusion:** Experimental determination of the resonance energy, particularly whether it lies below 200 keV, is crucial for determining the value of the branching ratio.

## I. INTRODUCTION

Exotic nuclei with unusual ratios of protons to neutrons can undergo a variety of decay modes [1, 2]. Occasionally, the decay probability for these rare processes such as the beta-delayed proton emission is unexpectedly high. The beta-delayed proton emission typically occurs in very proton-rich nuclei [3]. However, the emission of protons following beta decay is also energetically allowed for neutron-rich nuclei with neutrons bound by less than 782 keV [4]. The most promising candidate is  $^{11}\text{Be}$  [5]. The  $1/2^+$  ground state of  $^{11}\text{Be}$  is a one-neutron  $s$ -wave halo state [6], bound by only 501 keV [7].

The beta-delayed proton emission of  $^{11}\text{Be}$  was confirmed by experiments indirectly [8] and directly [9] with an unexpectedly high branching ratio. It can be explained by the decay proceeds through a proton resonance in  $^{11}\text{B}$ , located near the proton-emission threshold [10]. This resonance had not yet been discovered at that time. Its evidences were found later in experiments [11, 12]. The resonance was identified as the  $s$ -wave single-particle resonance [13].

In Ref. [9] that directly observed the proton emission in  $^{11}\text{Be}$  for the first time, the branching ratio is estimated as  $8.6 \times 10^{-6}$ . Theoretical calculations give smaller values [14–16]. In addition, the new experiment in Ref. [17]

raised the question of the upper limit of the branching ratio. According to Refs. [8, 17], this limit is determined to be  $2.2 \times 10^{-6}$ . The resonance parameters are important to determine the value of the branching ratio. However, the location of the resonance is still uncertain. In different experiments, its values are 171 keV [11], 197 keV [9], and 211 keV [12].

In the present work, the branching ratio is calculated within the potential model followed by Ref. [5]. We now take into account the near proton-emission threshold resonance [11, 12], and the spectroscopic factor. The single-particle bound and scattering potentials are obtained simultaneously within the Skyrme Hartree-Fock formalism. We use two overall scaling parameters for the potentials to give exactly the experimental values of the halo neutron separation energy and the location of the narrow resonance near the proton-emission threshold. The calculation method is valid for the studies of elastic scattering [13, 18–20] and radiative-capture reactions at keV energy [21–23]. In Ref. [13], it was applied to emphasize the single-particle properties of the resonance found in Refs. [11, 12, 24]. As we apply the same calculation to compute the branching ratio, we show the direct correlation between the resonance location and the branching ratio.

We demonstrate that the branching ratio exhibits a rapid variation when the resonance position shifts by just a few tens of keV. The estimated value  $8.6 \times 10^{-6}$  from Ref. [9] is consistent to the resonance location below 200 keV (197 keV [9]). The limit of  $2.2 \times 10^{-6}$  [8, 17] places the resonance at the energy above 200 keV (217 keV in

---

\* anhnl@hcmue.edu.vn

† lmbui@sdsu.edu

our calculation). The upper limit of the branching ratio may reach the order of  $10^{-5}$ .

An experiment measuring the resonance energy to ascertain whether it falls below 200 keV will be key to resolving the puzzle. From our analysis, the branching ratio is  $9 \times 10^{-6}$ . It is independent of the choice of the Skyrme forces. This value comes from the analysis with the resonance located at 182 keV, the spectroscopic factor of the neutron halo state being 0.51.

## II. METHOD OF CALCULATION

The beta decay of the halo neutron proceeds as

$${}^A_{Z+1}X \rightarrow {}^A_ZX + p + e^- + \bar{\nu}_e, \quad (1)$$

where the parent nucleus  ${}^A_{Z+1}X$  is understood as a system with a halo neutron that is quasi-bound in the core (daughter) nucleus  ${}^A_ZX$ .

The branching ratio ( $b_{\beta p}$ ) is given by

$$b_{\beta p} = \frac{WT_{1/2}}{\ln 2}, \quad (2)$$

where  $T_{1/2}$  is the half-life of the halo nucleus and  $W$  is the decay probability per unit time, defined as

$$W = \int_0^Q \frac{dW}{dE} dE, \quad (3)$$

where  $E$  is the relative energy of the proton-core system in the exit channel, and  $Q$  is the total energy available in the decay, expressed as

$$Q = (m_n - m_p - m_e)c^2 - S_n, \quad (4)$$

where  $m_n$ ,  $m_p$ , and  $m_e$  represent the neutron, proton, and electron masses, respectively, and  $S_n$  is the neutron separation energy of the halo nucleus. In the specific case of  ${}^{11}\text{Be} \rightarrow {}^{10}\text{Be} + p + e^- + \bar{\nu}_e$ ,  $S_n = 501$  keV and  $Q = 281$  keV.

The  $ft$  value for the contribution of both Fermi and Gamow-Teller transitions is given by

$$ft = \frac{K}{B_F + \lambda^2 B_{GT}}, \quad (5)$$

where  $K = 6144$  s, as reported in Refs. [1, 25]. The differential decay probability per unit time is given by [5, 26]

$$\frac{dW}{dE} = \frac{1}{2\pi^3} \frac{m_e c^2}{\hbar} G_\beta^2 f(Q - E) \left( \frac{dB_F}{dE} + \lambda^2 \frac{dB_{GT}}{dE} \right), \quad (6)$$

where  $G_\beta = 2.996 \times 10^{-12}$  is the dimensionless beta-decay constant, and  $\lambda = -1.268$  is the axial-to-vector coupling constant ratio. In Eq. (6), the Fermi integral  $f(Q - E)$  is computed over  $w_e$  which is the total energy

of the electron (in units of  $m_e c^2$ ) at a given phase-space point and is given by

$$f(w_0) = \int_1^{w_0} p_e w_e (w_0 - w_e)^2 F(Z, w_e) dw_e, \quad (7)$$

where  $p_e$  is the electron momentum, defined as  $p_e = \sqrt{w_e^2 - 1}$ . The total energy of the electron, including its rest mass, is  $w_0 = 1 + (Q - E)/(m_e c^2)$ . The Fermi function  $F(Z, w_e)$  accounts for the Coulomb interaction between the emitted electron and the charge of the daughter nucleus ( $Z = 4$ ). For low-energy beta decays, the Fermi function can be approximated by

$$F(Z, w_e) \approx \frac{2\pi\eta_e}{1 - \exp(-2\pi\eta_e)}, \quad (8)$$

where the Sommerfeld parameter  $\eta_e$  is defined as  $\eta_e = \alpha Z w_e / p_e$ , with  $\alpha = 1/137$  being the fine-structure constant.

The initial state  $i$  is a bound state where a neutron couples to the core nucleus  ${}^A_ZX$ . The final state is a scattering state involving the core and a proton. The orbital angular momenta of the relative motion in the initial and final states are denoted as  $\ell_i$  and  $\ell_f$ , respectively, while the total angular momenta are  $j_i$  and  $j_f$ .

The reduced decay probabilities for Fermi ( $B_F$ ) and Gamow-Teller ( $B_{GT}$ ) transitions are given by [5, 26]

$$\frac{dB_F}{dE} = \frac{1}{\hbar v} I_{if}^2(E), \quad \text{and} \quad \frac{dB_{GT}}{dE} = 3 \frac{dB_F}{dE}. \quad (9)$$

$E$  and  $v$  are the relative energy and velocity of the system in the scattering state, respectively,  $E = \mu v^2/2$ , and  $\mu$  is the reduced mass. As the final wave function is independent of  $j_f$ , the Gamow-Teller term simplifies to three times the Fermi term.

The key component is the overlap radial integral

$$I_{if}(E) = S_F^{1/2} \int_0^\infty \chi(E, r) \phi(r) dr. \quad (10)$$

The similar radial integral in Eq. (10) is successfully applied to study the magnetic dipole transition ( $M1$ ) in light nuclei at keV energy [23]. The  $s$ -wave functions  $\chi(E, r)$  and  $\phi(r)$  are obtained by solving the Schrödinger equations of the initial (bound) and final (scattering) states of neutrons ( $q = 0$ ) and protons ( $q = 1$ ), respectively. The two potentials are obtained within the Skyrme Hartree-Fock formalism

$$V_q(E, r) = \frac{m_q^*(r)}{m} \left\{ V_q^{\text{HF}}(r) + \frac{1}{2} \frac{d^2}{dr^2} \left( \frac{\hbar^2}{2m_q^*(r)} \right) - \frac{m_q^*(r)}{2\hbar^2} \left[ \frac{d}{dr} \left( \frac{\hbar^2}{2m_q^*(r)} \right) \right]^2 \right\} + \left[ 1 - \frac{m_q^*(r)}{m} \right] E. \quad (11)$$

The Hartree-Fock mean field  $V_q^{\text{HF}}(r)$  and the effective mass  $m_q^*(r)$  are obtained from the `skyrme_rpa` program [27]. The energy  $E$  can be either positive for the scattering state or negative for the bound state in Eq. (11). We

use the Skyrme forces SkM\* [28], SAMi-ISB [29], SLy4 [30], and SAMi [31] for illustration.

When using Eq. (11), the two nuclear potentials are adjusted by two overall scaling parameters  $\mathcal{N}_i$  and  $\mathcal{N}_f$  for the initial and final state, respectively. The parameter  $\mathcal{N}_i$  is fine-tuned to reproduce the separation energy of the halo neutron,  $S_n = 501$  keV, and the parameter  $\mathcal{N}_f$  is calibrated to the location of the resonance. Note that the overlap function in the study is different from the one in the radiative capture reaction by the fact that the initial and the final state are different particles. The many-body Coulomb potential is included for the proton case and kept unchanged. For the elastic scattering, the cross section is obtained by the standard matching method, and the width  $\Gamma_p$  is

$$\Gamma_p(E_R) = 2 \left[ \frac{d\delta(E)}{dE} \right]_{E=E_R}^{-1}, \quad (12)$$

where  $\delta$  is the phase shift and  $E_R$  is the resonance location.

Finally, the spectroscopic factor  $S_F$  in Eq. (10) is the percentage of the halo-neutron configuration in  $^{11}\text{Be}$ . It leads to a reduction in the branching ratio and an enhancement in the  $ft$  value. The spectroscopic factor  $S_F$  is 0.71 according to Ref. [6] which is fairly large. We use the smaller value of  $S_F = 0.51$  provided in Ref. [32] for all calculations.

TABLE I. Branching ratios obtained with and without calibrating to the exact resonance locations at 171 keV, 182 keV, and 211 keV. The spectroscopic factor  $S_F$  of the halo neutron state in  $^{11}\text{Be}$  is 0.51. The calculations with  $\mathcal{N}_f = 1$  are noted as ‘‘Untuned’’. When the factor  $\mathcal{N}_f$  is adjusted, all Skyrme forces give slightly different results. The upper limit of the branching ratio may reach the order of  $10^{-5}$ .

Skyrme	SkM*	SAMi-ISB	SLy4	SAMi
Untuned	$23.2 \times 10^{-6}$	$37.0 \times 10^{-6}$	$2.26 \times 10^{-9}$	$4.89 \times 10^{-8}$
171 keV	$13.2 \times 10^{-6}$	$12.9 \times 10^{-6}$	$12.9 \times 10^{-6}$	$12.9 \times 10^{-6}$
182 keV	$8.91 \times 10^{-6}$	$8.98 \times 10^{-6}$	$8.97 \times 10^{-6}$	$9.05 \times 10^{-6}$
211 keV	$2.86 \times 10^{-6}$	$2.90 \times 10^{-6}$	$2.88 \times 10^{-6}$	$2.89 \times 10^{-6}$

### III. RESULTS AND DISCUSSION

In Fig. 1, we show our results without the calibration of the location of the resonance,  $\mathcal{N}_f = 1$ . Figures 1(a) and (b) show the cross sections at a scattering angle of  $180^\circ$  and the corresponding  $s$ -wave phase shifts, respectively. Without the calibration, we observed the resonances in the cases of SkM\* and SAMi-ISB forces. We also see that the resonance with SLy4 force is located below the  $p+^{10}\text{Be}$  threshold, while the one with SAMi is at 500 keV which is higher than the total energy  $Q$

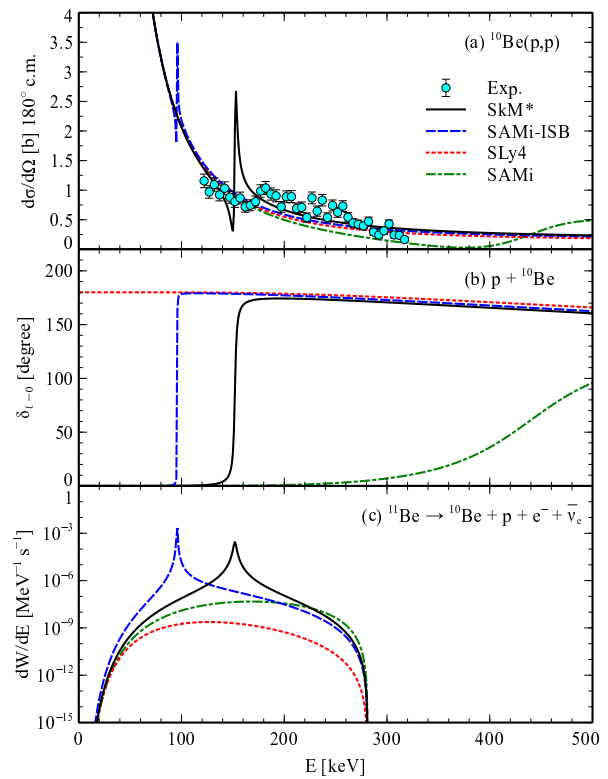


FIG. 1. (a) Excitation functions in the center-of-mass frame for  $^{10}\text{Be}(p,p)$  scattering using different forces without adjusting  $\mathcal{N}$ . The SkM\* and SAMi-ISB forces show the resonances in the experimental region [11, 12]. (b) Phase shifts for the  $s$ -wave in the  $p+^{10}\text{Be}$  system. (c) The corresponding result for the decay probability distribution per second.

in decay. Figure 1(c) shows the branching ratios, interpreted as the areas under the curves below  $Q = 281$  keV. Note that only when the resonance appears below 281 keV, the branching ratio is enhanced dramatically. The presence of a resonance below this energy can increase the branching ratio by up to three orders of magnitude compared to cases without such a resonance. The values of the branching ratio are given in Table I, noted as ‘‘Untuned’’, indicating that  $\mathcal{N}_f = 1$ .

When the calibration is applied to fix the location of the resonance, the results remain nearly identical with all Skyrme forces in the study. The values of  $\mathcal{N}_i$  and  $\mathcal{N}_f$  as shown in Table II are close to unity. All  $\mathcal{N}_i$  are slightly larger than unity showing that the energy of  $s_{1/2}$  state without the fine-tuning is positive and very close to zero. A minimal adjustment can make this state bound and reproduce the neutron-halo properties of  $^{11}\text{Be}$ . The sensitivity of the location of the resonance, particularly in the energy range that strongly and directly affects the branching ratio, to the value of  $\mathcal{N}_f$  was discussed in Ref. [13].

The evidence of the near-threshold resonance in Refs. [11, 12] confirmed the mechanism of the enhanced branching ratio. However, the experimental uncertainties in these studies are significant, with error bars being

TABLE II. Parameters  $\mathcal{N}_i$  and  $\mathcal{N}_f$  used to reproduce the neutron separation energy  $S_n$  in  $^{11}\text{B}$ , and the resonance location at 182 keV, respectively.

Skyrme	SkM*	SAMi-ISB	SLy5	SAMi
$\mathcal{N}_i$	1.086	1.141	1.149	1.125
$\mathcal{N}_f$	0.997	0.991	0.978	1.028

$\pm 20$  keV [11] and  $\pm 40$  keV [12]. As shown in our analysis in Table I and illustrated in Fig. 2, the value of the branching ratio is strongly sensitive to the location of the resonance.

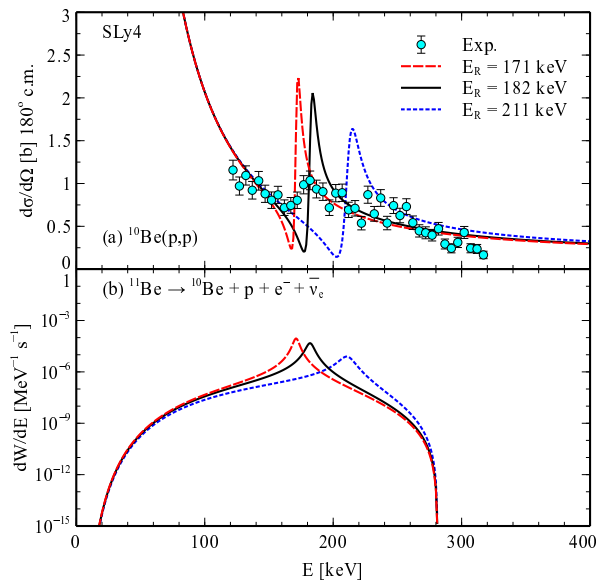


FIG. 2. (a) The excitation functions in the center-of-mass frame for  $^{10}\text{Be}(p,p)$ . (b) The decay probability distribution per second for SLy4 fitted to the exact resonance locations at 171 keV [11] and 211 keV [12].

Note that the branching ratio in Ref. [9] is  $8.6 \times 10^6$  based on the overlap  $I = 53$ , and an  $S_F = 0.34$ . In Table III, we show the value of the overlap  $I$  and the width of the resonance from our calculations. The values of  $B_F$  and  $B_{GT}$  are also given. We provide a more consistent and microscopic analysis but still support the branching ratio from this estimation. The branching ratio is in the order of  $10^{-5}$  if the resonance is at 171 keV. The smaller value of the branching ratio corresponds to the resonance above 200 keV. For example, if the resonance is at 217 keV, the branching ratio is  $2.2 \times 10^6$  as shown in Fig. 3. Finally, our analysis gives the value of the branching ratio as  $9 \times 10^6$ .

TABLE III. The overlap integrals  $I_{if}$ ,  $B_F$  and  $B_{GT}$  transitions,  $\log(ft)$  values, and the widths of single-particle resonances  $\Gamma_p$  computed with SLy4 force.

$E_R$ [keV]	171	182	211
$\Gamma_p$ [keV]	4.738	6.249	11.905
$I_{if}$	19.27	17.02	12.82
$B_F$	1.364	1.353	1.307
$B_{GT}$	4.092	4.061	3.920
$\log(ft)$	2.621	2.628	2.659

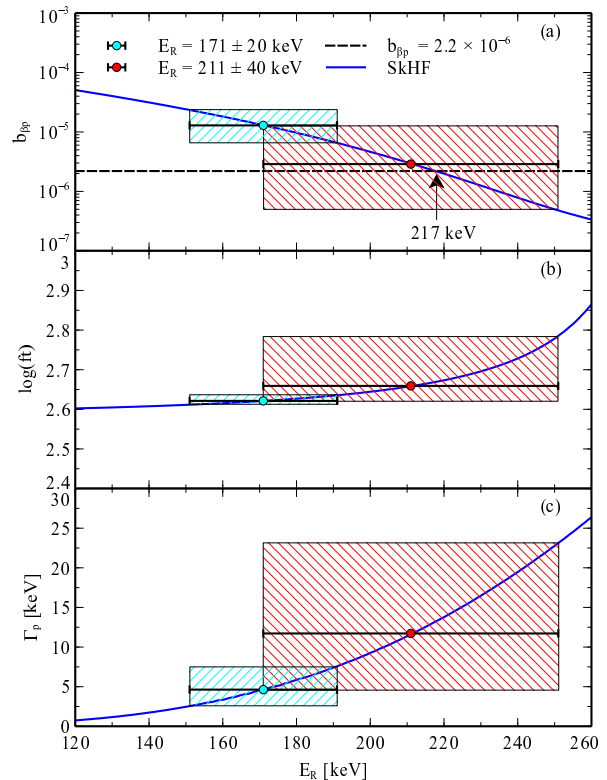


FIG. 3. The branching ratios  $b_{\beta p}$ , logarithm of  $ft$  values, and proton-decay width  $\Gamma_p$  as functions of resonance locations  $E_R$  with the error bar. The value of  $2.2 \times 10^{-6}$  reported in Refs. [8, 17] places the resonance at 217 keV.

#### IV. CONCLUSION

Our result strengthens the link between low-energy proton elastic scattering, a nuclear process governed by strong interactions, and the branching ratio of beta-delayed proton emission, a weak interaction process. This connection highlights the interplay between nuclear structure and weak decay channels, offering deeper insights into how nuclear and weak forces influence each other at low energy. The Skyrme Hartree-Fock formalism provides a consistent microscopic approach to the potential model.

As suggested in Ref. [17], further studies are needed to

verify the existence of the  $\beta p$  decay branch of  $^{11}\text{Be}$  and to clarify the puzzle of its strength. Determining the resonance location with greater precision is crucial to solving the puzzle [24]. High-profile FRIB experiments with attention to near-threshold physics are now available [33].

## ACKNOWLEDGEMENT

We thank Prof. Calvin Johnson (SDSU) for discussing and carefully reading the manuscript. BML is supported by the U.S. Department of Energy, under Award Number DE-NA0004075.

- 
- [1] M. Pfützner, M. Karny, L. V. Grigorenko, and K. Riisager, Radioactive decays at limits of nuclear stability, *Rev. Mod. Phys.* **84**, 567 (2012).
- [2] A. Volya and V. Zelevinsky, Puzzles of exotic decay processes, *Few-Body Systems* **65**, 43 (2024).
- [3] J. C. Batchelder, Recommended values for  $\beta^+$ -delayed proton and  $\alpha$  emission, *At. Data Nucl. Data Tables* **132**, 101323 (2020).
- [4] M. Horoi and V. Zelevinsky, in: April Meeting, American Physical Society, Philadelphia, PA, 2003, abstract U10.001 (2003).
- [5] D. Baye and E. M. Tursunov,  $\beta$  delayed emission of a proton by a one-neutron halo nucleus, *Phys. Lett. B* **696**, 464 (2011).
- [6] K. T. Schmitt, K. L. Jones, A. Bey, S. H. Ahn, D. W. Bardayan, J. C. Blackmon, S. M. Brown, K. Y. Chae, K. A. Chipps, J. A. Cizewski, K. I. Hahn, J. J. Kolata, R. L. Kozub, J. F. Liang, C. Matei, M. Matoš, D. Matyas, B. Moazen, C. Nesaraja, F. M. Nunes, P. D. O'Malley, S. D. Pain, W. A. Peters, S. T. Pittman, A. Roberts, D. Shapira, J. F. Shriner, M. S. Smith, I. Spassova, D. W. Stracener, A. N. Villano, and G. L. Wilson, Halo Nucleus  $^{11}\text{Be}$ : A Spectroscopic Study via Neutron Transfer, *Phys. Rev. Lett.* **108**, 192701 (2012).
- [7] J. H. Kelley, E. Kwan, J. E. Purcell, C. G. Sheu, and H. R. Weller, Energy levels of light nuclei A=11, *Nucl. Phys. A* **880**, 88 (2012).
- [8] K. Riisager, M. J. G. Borge, J. A. Briz, M. Carmona-Gallardo, O. Forstner, L. M. Fraile, H. O. U. Fynbo, A. G. Camacho, J. G. Johansen, B. Jonson, M. V. Lund, J. Lachner, M. Madurga, S. Merchel, E. Nacher, T. Nilsson, P. Steier, O. Tengblad, and V. Vedia, Search for beta-delayed proton emission from  $^{11}\text{Be}$ , *Eur. Phys. J. A* **56**, 100 (2020).
- [9] Y. Ayyad, B. Olaizola, W. Mittig, G. Potel, V. Zelevinsky, M. Horoi, S. Beceiro-Novo, M. Alcorta, C. Andreoiu, T. Ahn, M. Anholm, L. Atar, A. Babu, D. Bazin, N. Bernier, S. S. Bhattacharjee, M. Bowry, R. Caballero-Folch, M. Cortesi, C. Dalitz, E. Dunling, A. B. Garnsworthy, M. Holl, B. Kootte, K. G. Leach, J. S. Randhawa, Y. Saito, C. Santamaria, P. Šiurytė, C. E. Svensson, R. Umashankar, N. Watwood, and D. Yates, Direct observation of proton emission in  $^{11}\text{Be}$ , *Phys. Rev. Lett.* **123**, 082501 (2019).
- [10] K. Riisager, O. Forstner, M. J. G. Borge, J. A. Briz, M. Carmona-Gallardo, L. M. Fraile, H. Fynbo, T. Giles, A. Gottberg, A. Heinz, J. G. Johansen, B. Jonson, J. Kurcewicz, M. V. Lund, T. Nilsson, G. Nyman, E. Rapisarda, P. Steier, O. Tengblad, R. Thies, and S. R. Winkler,  $^{11}\text{Be}(\beta p)$ , a quasi-free neutron decay?, *Phys. Lett. B* **732**, 305 (2014).
- [11] Y. Ayyad, W. Mittig, T. Tang, B. Olaizola, G. Potel, N. Rijal, N. Watwood, H. Alvarez-Pol, D. Bazin, M. Caamaño, J. Chen, M. Cortesi, B. Fernández-Domínguez, S. Giraud, P. Gueye, S. Heinitz, R. Jain, B. P. Kay, E. A. Maugeri, B. Monteagudo, F. Ndayisabye, S. N. Paneru, J. Pereira, E. Rubino, C. Santamaria, D. Schumann, J. Surbrook, L. Wagner, J. C. Zamora, and V. Zelevinsky, Evidence of a near-threshold resonance in  $^{11}\text{B}$  relevant to the  $\beta$ -delayed proton emission of  $^{11}\text{Be}$ , *Phys. Rev. Lett.* **129**, 012501 (2022).
- [12] E. Lopez-Saavedra, S. Almaraz-Calderon, B. W. Asher, L. T. Baby, N. Gerken, K. Hanselman, K. W. Kemper, A. N. Kuchera, A. B. Morelock, J. F. Perello, E. S. Temanson, A. Volya, and I. Wiedenhöver, Observation of a near-threshold proton resonance in  $^{11}\text{B}$ , *Phys. Rev. Lett.* **129**, 012502 (2022).
- [13] N. Le Anh, B. Minh Loc, N. Auerbach, and V. Zelevinsky, Single-particle properties of the near-threshold proton-emitting resonance in  $^{11}\text{B}$ , *Phys. Rev. C* **106**, L051302 (2022).
- [14] W. Elkamhawy, Z. Yang, H.-W. Hammer, and L. Platter,  $\beta$ -delayed proton emission from  $^{11}\text{Be}$  in effective field theory, *Phys. Lett. B* **821**, 136610 (2021).
- [15] M. C. Atkinson, P. Navrátil, G. Hupin, K. Kravvaris, and S. Quaglioni, Ab initio calculation of the  $\beta$  decay from  $^{11}\text{Be}$  to a  $^{10}\text{Be} + p$  resonance, *Phys. Rev. C* **105**, 054316 (2022).
- [16] W. Elkamhawy, H.-W. Hammer, and L. Platter, Weak decay of halo nuclei, *Phys. Rev. C* **108**, 015501 (2023).
- [17] N. Sokołowska, V. Guadilla, C. Mazzocchi, R. Ahmed, M. J. G. Borge, G. Cardella, A. A. Ciemny, L. G. Cosentino, E. De Filippo, V. Fedosseev, A. Fijałkowska, L. M. Fraile, E. Geraci, A. Giska, B. Gnoffo, C. Granados, Z. Janas, L. Janiak, K. Johnston, G. Kamiński, A. Korgul, A. Kubiela, C. Maiolino, B. Marsh, N. S. Martorana, K. Miernik, P. Molkanov, J. D. Ovejás, E. V. Pagano, S. Pirrone, M. Pomorski, A. M. Quynh, K. Riisager, A. Russo, P. Russotto, A. Świercz, S. Viñals, S. Wilkins, and M. Pfützner (ISOLDE Collaboration), Decay study of  $^{11}\text{Be}$  with an optical time-projection chamber, *Phys. Rev. C* **110**, 034328 (2024).
- [18] C. B. Dover and N. Van Giai, Low-energy neutron scattering by a Hartree-Fock field, *Nucl. Phys. A* **177**, 559 (1971).
- [19] C. B. Dover and N. Van Giai, The nucleon-nucleus potential in the Hartree-Fock approximation with Skyrme's interaction, *Nucl. Phys. A* **190**, 373 (1972).
- [20] N. Le Anh, Y.-h. Song, and B. Minh Loc, Proton  $s$ -resonance states of  $^{12}\text{C}$  and  $^{14,15}\text{O}$  within the Skyrme Hartree-Fock mean-field framework, *Phys. Rev. C* **107**, 034604 (2023).
- [21] N. Le Anh and B. Minh Loc, Bound-to-continuum potential model for the  $(p, \gamma)$  reactions of the CNO nucleosynthesis cycle, *Phys. Rev. C* **103**, 035812 (2021).

- [22] N. Le Anh, P. Nhut Huan, and B. Minh Loc, Potential model within a bound-to-continuum approach for low-energy nucleon radiative capture by  $^{12}\text{C}$  and  $^{16}\text{O}$ , *Phys. Rev. C* **104**, 034622 (2021).
- [23] N. Le Anh and B. Minh Loc, Low-energy  $^7\text{Li}(n, \gamma)^8\text{Li}$  and  $^7\text{Be}(p, \gamma)^8\text{B}$  radiative capture reactions within the Skyrme Hartree-Fock approach, *Phys. Rev. C* **106**, 014605 (2022).
- [24] Y. Ayyad, B. Olaizola, W. Mittig, G. Potel, V. Zelevinsky, M. Horoi, S. Beceiro-Novo, M. Alcorta, C. Andreoiu, T. Ahn, M. Anholm, L. Atar, A. Babu, D. Bazin, N. Bernier, S. S. Bhattacharjee, M. Bowry, R. Caballero-Folch, M. Cortesi, C. Dalitz, E. Dunling, A. B. Garnsworthy, M. Holl, B. Kootte, K. G. Leach, J. S. Randhawa, Y. Saito, C. Santamaria, P. Šiurytė, C. E. Svensson, R. Umashankar, N. Watwood, and D. Yates, Erratum: Direct observation of proton emission in  $^{11}\text{Be}$  [phys. rev. lett. 123, 082501 (2019)], *Phys. Rev. Lett.* **124**, 129902 (2020).
- [25] I. S. Towner and J. C. Hardy, The evaluation of  $V_{ud}$  and its impact on the unitarity of the Cabibbo–Kobayashi–Maskawa quark-mixing matrix, *Rep. Prog. Phys.* **73**, 046301 (2010).
- [26] D. Baye, P. Descouvemont, and E. M. Tursunov, Unique decay process:  $\beta$ -delayed emission of a proton and a neutron by the  $^{11}\text{Li}$  halo nucleus, *Phys. Rev. C* **82**, 054318 (2010).
- [27] G. Colò, L. Cao, N. Van Giai, and L. Capelli, Self-consistent RPA calculations with Skyrme-type interactions: The `skyrme_rpa` program, *Comput. Phys. Commun.* **184**, 142 (2013).
- [28] J. Bartel, P. Quentin, M. Brack, C. Guet, and H.-B. Håkansson, Towards a better parametrisation of Skyrme-like effective forces: A critical study of the SkM force, *Nucl. Phys. A* **386**, 79 (1982).
- [29] X. Roca-Maza, G. Colò, and H. Sagawa, Nuclear Symmetry Energy and the Breaking of the Isospin Symmetry: How Do They Reconcile with Each Other?, *Phys. Rev. Lett.* **120**, 202501 (2018).
- [30] E. Chabanat, P. Bonche, P. Haensel, J. Meyer, and R. Schaeffer, A Skyrme parametrization from subnuclear to neutron star densities Part II. Nuclei far from stabilities, *Nucl. Phys. A* **635**, 231 (1998).
- [31] X. Roca-Maza, G. Colò, and H. Sagawa, New Skyrme interaction with improved spin-isospin properties, *Phys. Rev. C* **86**, 031306 (2012).
- [32] J. Lee, M. B. Tsang, and W. G. Lynch, Neutron spectroscopic factors from transfer reactions, *Phys. Rev. C* **75**, 064320 (2007).
- [33] B. A. Brown, A. Gade, S. R. Stroberg, J. Escher, K. Fosse, P. Giuliani, C. R. Hoffman, W. Nazarewicz, C.-Y. Seng, A. Sorensen, N. Vassh, D. Bazin, K. W. Brown, M. A. Capri, H. Crawford, P. Danielewicz, C. Drischler, R. F. G. Ruiz, K. Godbey, R. Grzywacz, J. W. Holt, H. Iwasaki, D. Lee, S. M. Lenzi, S. Liddick, R. Lubna, A. O. Macchiavelli, G. M. Pinedo, A. McCoy, A. Mercenne, K. Minamisono, B. Monteagudo, P. Navratil, R. Ringle, G. Sargsyan, H. Schatz, M.-C. Spieker, A. Volya, R. G. T. Zegers, V. Zelevinsky, and X. Zhang, Motivations for Early High-Profile FRIB Experiments (2024), arXiv:2410.06144 [nucl-th].